Thermodynamic Density of States of Two-Dimensional GaAs Systems near the Apparent Metal-Insulator Transition

G. Allison,[1] E. A. Galaktionov,[1] A. K. Savchenko,[1] S. S. Safonov,[1] M. M. Fogler,[2] M. Y. Simmons,[3,*] and D. A. Ritchie[3]

[1]*School of Physics, University of Exeter, Exeter EX4 4QL, United Kingdom*
[2]*Department of Physics, University of California San Diego, La Jolla, California 92093, USA*
[3]*Cavendish Laboratory, University of Cambridge, Madingley Road, Cambridge CB3 0HE, United Kingdom*
(Received 24 December 2005; published 2 June 2006)

We perform combined resistivity and compressibility studies of two-dimensional hole and electron systems which show the apparent metal-insulator transition—a crossover in the sign of $\partial R/\partial T$ with changing density. No thermodynamic anomalies have been detected in the crossover region. Instead, despite a tenfold difference in r_s, the compressibility of both electrons and holes is well described by the theory of nonlinear screening of the random potential. We show that the resistivity exhibits a scaling behavior near the percolation threshold found from analysis of the compressibility. Notably, the percolation transition occurs at a much lower density than the crossover.

The apparent metal-insulator transition (MIT) in high-mobility two-dimensional systems remains a topic of fundamental interest [1] and continuing debate [2]. The anomaly of these systems is exemplified by the existence of a narrow range of carrier densities around $n = n_c$ where the slope of the temperature dependence of the resistance, $\partial R/\partial T$, changes its sign. To unravel a complex interplay between interactions and disorder in this phenomenon, it is essential to combine transport measurements with other experimental probes, in particular, measurements of the thermodynamic density of states [also referred to as the charge compressibility [3,4]] $\chi = dn/d\mu$, where μ is the chemical potential. There have been only a few measurements of χ near the apparent MIT [5–7], among which work [5] on a 2D hole gas with large values of the Coulomb interaction parameter $r_s \equiv 1/\sqrt{\pi n a_B^2} \approx 5$–16 has attracted much attention. (Here $a_B = 18$ Å is the effective Bohr radius for the hole mass of $0.38m_0$.) In their experiments done at $T = 0.3$–1.3 K the authors of Ref. [5] found that the inverse compressibility $\chi^{-1}(n)$ has a minimum which is positioned exactly at n_c. This was interpreted as a thermodynamic signature of an interaction-driven phase transition discussed in theoretical works [8,9].

An alternative explanation of the minimum of $\chi^{-1}(n)$ can be based on the nonlinear screening theory (NST) [10–13] that emphasizes the role of disorder. The basic premise of the NST is that a low-density metal is unable to screen fluctuations of potential, so that depletion regions with vanishingly small local density appear and grow as n decreases. The NST predicts that $\chi^{-1}(n)$ has a minimum at $n = n_m$ (determined by disorder), and a rapid upturn to positive values at $n < n_m$.

This theory also predicts a percolation threshold at $n = n_p$ [11], where $n_p \approx n_m/3$ in typical GaAs systems [13]. There have been suggestions, based on the conductance scaling, that the percolation transition is closely related to

the change in the sign of $\partial R/\partial T$ [12,14,15]. [The existence of the percolative MIT in 2D GaAs structures was proposed earlier in [11].]

In this work we use combined compressibility and conductance measurements to shed light on the origin of the apparent MIT in 2D hole gases (2DHGs) with large interactions between the carriers—a problem widely debated over the last few years [16–18]. We find no signature of a critical behavior of $\chi^{-1}(n)$ near the apparent MIT. We do find evidence for the percolation transition, but it occurs at a concentration much lower than n_c. Finally, the NST provides a quantitatively accurate description of both the measured compressibility and the position of the percolation point. As for the sign change of $\partial R/\partial T$, we surmise that in our 2DHG samples it is most likely caused by an interplay of different scattering mechanisms [19–21], similar to 2D electron gas (2DEG).

Two types of system have been examined: a 2DEG with $r_s = 1$–4 and a 2DHG with $r_s = 10$–35. We find *no* relation between the position n_m of the minimum in χ^{-1} and the position n_c of the MIT—the two densities can differ by a factor of 2 and, furthermore, their ratio is sample and cooldown dependent. The $\chi^{-1}(n)$ dependence fits the NST [13] predictions very well for *both* carrier types. We show that in some range of T the dependence of the conductance of both systems on carrier density fits the usual percolation scaling ansatz. The percolation threshold found agrees with the prediction from the analysis of the compressibility in terms of the NST. However, its density is significantly lower than the crossover density n_c, which makes a direct, universal connection between the apparent MIT (the sign change of $\partial R/\partial T$) and percolation doubtful.

Our 2DEG structures E01 and E02 contain two GaAs quantum wells of width $w = 200$ Å separated by a 200 Å and 300 Å-thick AlGaAs barrier, respectively, Fig. 1. The top-layer mobility at the highest density is 5×10^5 cm^2/V s for E01 and 8×10^5 cm^2/V s for E02. The
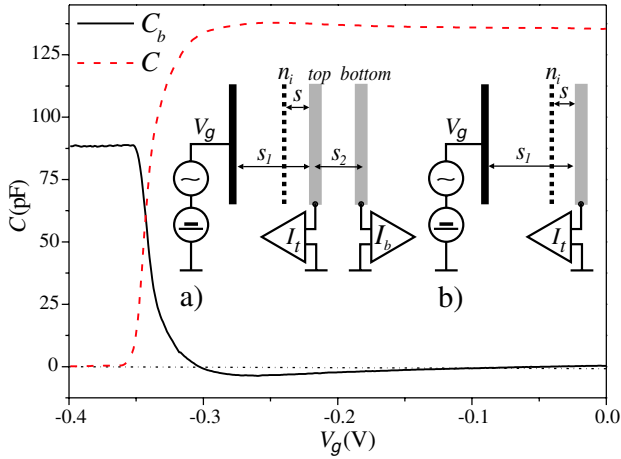
FIG. 1 (color online). Capacitance of a double-layer 2DEG structure E01 measured simultaneously by two methods: C_b—field penetration, C—capacitance; $T = 4.2$ K, $f = 4$ Hz. Inset: diagrams of capacitance measurements in (a) double- and (b) single-layer structures.

2DHG samples H03 and H05 with mobility 4.7×10^5 cm^2/V s and 5.6×10^5 cm^2/V s, respectively, are formed in standard single-layer AlGaAs/GaAs heterostructures with Au gates.

The resistance as a function of gate voltage, V_g, is measured at $T = 0.03$–10 K, in a similar way to [16], and the relation between V_g and n is established by the Hall effect. The position of n_c is determined at the lowest temperature of the compressibility measurements, $T = 0.26$ K. The compressibility is found to be temperature independent in the range 0.26–1.5 K for 2DHGs and 0.26–5 K for 2DEGs. The compressibility and conductance measurements have been repeated several times, one after another, to confirm that there is no drift in the structure. The compressibility is determined using two techniques—the "capacitance" and the "field penetration", Fig. 1.

Capacitance method.—Here the ac voltage $\tilde{V}_g = 2$ mV of frequency $f = 1$–100 Hz is applied to the gate and the 90° phase-shifted current $\tilde{I}$ in the probed layer is measured (Fig. 1, inset), yielding the capacitance $C = \tilde{I}/2\pi f \tilde{V}_g$. Instead of χ we discuss the quantity which is a measure of inverse compressibility: the Thomas-Fermi screening radius $d \equiv (\varepsilon\varepsilon_0/e^2)\chi^{-1}$ [3]. It is easy to show that d is related to C by the formula $d = \varepsilon\varepsilon_0 A(C^{-1} - C_0^{-1})/(1 + \gamma^{-1})$, where A is the gated area and $C_0 = \varepsilon\varepsilon_0 A/s_1$ is the geometric capacitance between the gate and the probed 2D layer, Fig. 1. In a double-layer structure, where the "probed" 2D layer is the top quantum well, the factor $\gamma \equiv (d_b + s_2 + w)/s_1$ accounts for the electrostatic interaction between the two layers [3]. Here s_2 is the separation between the centers of the quantum wells and $d_b \approx a_B/4 \ll s_2 + w$ is the screening radius of the bottom layer. In a single-layer structure $s_2 \to \infty$ and the correction γ^{-1} is set to zero.

Field-penetration method.—In this technique the compressibility of the top layer is found from the capacitance C_b between the gate and the bottom layer. The measured capacitive current $\tilde{I}_b$ is caused by the electric field penetrating through the top layer in proportion to its χ^{-1}. Once $C_b(V_g)$ is found, the screening radius d is calculated using Eqs. (7)–(9) of Ref. [3].

In real 2D systems there is a change in the transverse confinement (and the corresponding subband energy) with varying n. This gives a small contribution Δd_{sub} to d whose sign and magnitude depend on the structure and the method of capacitance measurement. To compare the results obtained in different experimental situations, we subtract this contribution and discuss the quantity $d^* = d - \Delta d_{\text{sub}}$. The value of Δd_{sub} is of the order of the 2D layer thickness and is calculated by a perturbation theory. For a single-layer heterostructure $\Delta d_{\text{sub}} = 0.46(a_B/n)^{1/3}$ [22]. For double-layer (quantum well) structures we compute Δd_{sub} using the infinite square-well approximation, similarly to Ref. [23]. This gives for the capacitance method $\Delta d_{\text{sub}} = +0.3967w(1 - 0.0544\lambda)$ in the thin-well limit, $\lambda = nw^3/a_B \ll 1$. In the field-penetration technique $\Delta d_{\text{sub}} = -0.1033w(1 - 0.1148\lambda)$; cf. Ref. [3].

In Fig. 2 we present d^* for sample E01 found from both the capacitance and the field-penetration methods. The field-penetration technique is more accurate than the capacitance technique at large n, because in this method the subtraction of the geometric term C_0 is obviated. However, at low densities around the minimum in χ^{-1} the contribu-
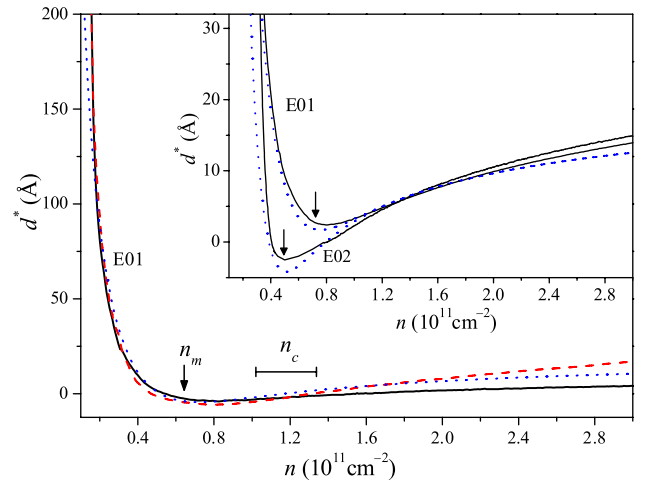

FIG. 2 (color online). d^* for 2DEG structure E01 with $s = 200$ Å, $s_1 = 700$ Å, $s_2 = 400$ Å. Solid lines are the results of the field-penetration method, dashed line—the capacitance method. Dotted line—the NST theory with $n_i = 1.2 \times 10^{11}$ cm^{-2}. [The donor concentration found from $\tau_q(n)$ is $n_i^\tau = 2.3 - 4.5 \times 10^{11}$ cm^{-2}, while the maximum concentration of (uncorrelated) donors is $n_i^G = 9.0 \times 10^{11}$ cm^{-2}.] Inset: comparison with 2DEG structure E02 ($s = 400$ Å, $s_1 = 900$ Å, $s_2 = 500$ Å), where $n_i = 2.2 \times 10^{11}$ cm^{-2} and $n_i^\tau = 3 - 4.5 \times 10^{11}$ cm^{-2}, while $n_i^G = 11 \times 10^{11}$ cm^{-2}).

tion C_0 is less important, and one can see that the two methods give nearly identical results.

Now we turn to the comparison of the results with the nonlinear screening theory. This theory predicts:

$$d^* = (a_B/4) + \Delta d_{ex} + \Delta d_{cor} + \Delta d_{dis}. \tag{1}$$

The first term in Eq. (1) is due to the single-particle density of states (kinetic energy) of the 2D carriers. The correction $\Delta d_{ex} = -(8\pi^3 n)^{-1/2}$ comes from the exchange interaction. Another negative contribution is due to correlations between the carriers: $\Delta d_{cor} = (\varepsilon\varepsilon_0/e^2)d^2(nE_c)/dn^2$, where the correlation energy per particle E_c is computed according to Ref. [24]. As the carrier density decreases, Δd_{ex} and Δd_{cor} cause a change in the sign of d from positive to negative—the effect seen experimentally [3,5,7]. Disorder, however, brings a positive contribution, Δd_{dis}, responsible for the upturn of χ^{-1} at low densities [13]:

$$\Delta d_{dis} = \frac{3\sqrt{2}}{32\pi^2}\frac{(0.3 + \eta)s}{0.036\eta + 0.12\eta^2 + \eta^3}\exp(-4\pi\eta^2), \tag{2}$$

where $\eta \equiv ns/\sqrt{n_i}$, s is the spacer, and n_i is the effective 2D concentration of dopants (an adjustable parameter, see below).

Equation (2) was derived assuming that disorder is produced by a δ-doped layer of *uncorrelated* dopants with a two-dimensional concentration n_i [13]. The samples in this work have three-dimensional doping. It can be shown that the impurities closest to the 2D layer have the greatest effect on χ, and therefore Eq. (2) is still valid provided one uses an effective n_i. Unfortunately, n_i cannot be determined in a simple way because not all impurities can be ionized and also because of existing correlations in their positions [25]. Both factors reduce the effective n_i [11] compared to a naïve estimate based on the total number of impurities known from the growth conditions (denoted here by n_i^G). A better estimate of n_i is deduced from the quantum lifetime τ_q. We have found $\tau_q(n)$ from the analysis of the Shubnikov–de Haas effect and determined the effective concentration n_i^τ according to Ref. [20]—it turns out to be 3–5 times smaller than n_i^G.

The dotted line in Fig. 2 is the best fit by Eq. (1) for structure E01, with n_i found to be close to n_i^τ. Good agreement with Eq. (1) where n_i is close to n_i^τ has also been obtained for E02—the inset compares the results for the two 2DEG structures. The latter has a larger spacer and in agreement with the NST the $\chi^{-1}(n)$ minimum, $n_m \approx 0.38n_i^{1/2}/s$, is shifted to lower n. The position of the minimum in $\chi^{-1}(n)$, indicated by an arrow, is found from the fitted curve with an error of $\lesssim 2\%$. (Inaccuracy of the calculation of Δd_{sub} has an even smaller effect on the position of n_m.) The range of densities where $\partial R/\partial T$ changes its sign is indicated in Fig. 2 by n_c. It is seen that the crossover in $R(T)$ occurs at higher densities than the minimum in $\chi^{-1}(n)$.

Figure 3 shows the results for 2DHG samples H03 (two cooldowns) and H05. The dotted lines are best fits to Eq. (1) with parameters n_i consistent with our analysis of $\tau_q(n)$. In the second cooldown the upturn of d^* occurs at higher densities and the obtained n_i is also larger, i.e., the sample in this cooldown is more disordered. This supports the notion of correlations among the impurities since these are known to depend on thermal cycling [25]. As in the 2DEG structures, the apparent MIT region n_c does not overlap with n_m, although here $n_c < n_m$. This is not surprising because of the difference in the contributions to $R(T)$ of electrons and holes that determine the position of n_c. The same conclusion that $n_c < n_m$ was drawn for another studied 2DHG sample (H06, not shown).

To understand the relation between the apparent MIT and percolation in 2DHGs, we have attempted to extract the percolation threshold n_p^σ from the fit of the conductance to $\sigma(n) = \alpha(n - n_p^\sigma)^t$ following the procedure in [14,15,18]. Figure 4 shows the results with the exponent $t = 2.1 \pm 0.1$ at $T = 0.26$ K for both electrons and holes, which is close to that in works [15,18]. For the 2DHGs the exponent decreases with decreasing temperature to $t = 1.6 \pm 0.1$, which is close to $t = 1.31$ expected for classical percolation [26]. Notably, the value of the percolation threshold is significantly lower than n_c: $n_c/n_p^\sigma = 2.9$ for H03 and $n_c/n_p^\sigma = 2.1$ for H05. Therefore, we surmise that the apparent MIT is not due to percolation but, similar to 2DEGs [19], is due to an interplay of the "metallic" T dependence caused by phonon scattering and Fermi-liquid corrections to impurity scattering, and the "insulating" dependence caused by localization [16,17,20,21].
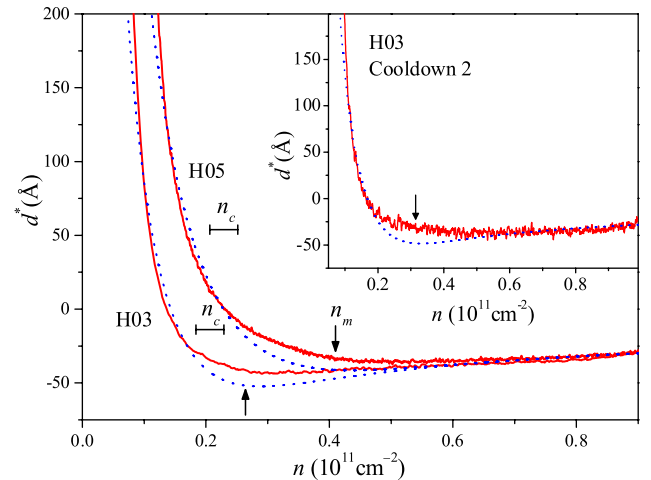

FIG. 3 (color online). d^* for 2DHG structures H03 and H05 with $s = 500$ Å and $s_1 = 2670$ Å, obtained by the capacitance method. Dotted lines—NST theory. The dopant concentrations for H03 are: $n_i = 1 \times 10^{11}$ cm^{-2}, $n_i^\tau = 1.1 - 2.2 \times 10^{11}$ cm^{-2} and $n_i^G = 5.6 \times 10^{11}$ cm^{-2}. The minimum for H05 ($n_i = 2.4 \times 10^{11}$ cm^{-2}, $n_i^G = 5.6 \times 10^{11}$ cm^{-2}) is shifted to larger n. Inset: d^* for H03 (cooldown 2), $n_i = 1.5 \times 10^{11}$ cm^{-2} and $n_i^G = 5.6 \times 10^{11}$ cm^{-2}.
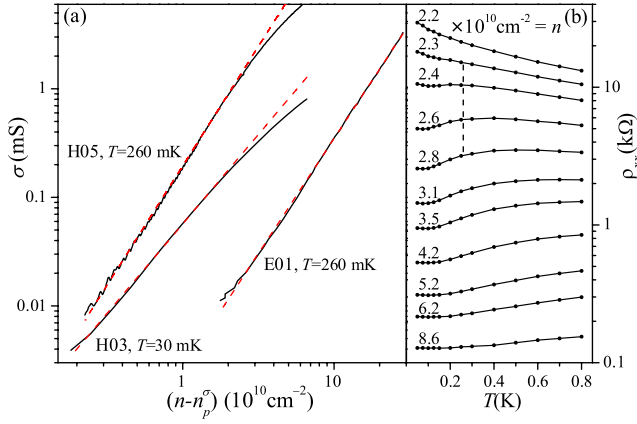
FIG. 4 (color online).   (a) Fits of the conductance to $\sigma(n) = \alpha(n - n_p^\sigma)^t$. (b) An example of the temperature dependence of the resistivity of H03 structure. The range of n_c in this cooldown is indicated by the dotted line.

We want to stress, however, that using the percolation scaling in a quantum system requires justification. One can rationalize this procedure by arguing that the percolation concept can apply in some intermediate range of T, high enough to preempt localization at $n > n_p^\sigma$ yet low enough to inhibit thermal activation at $n < n_p^\sigma$. Another point of concern is that the scaling is observed over a broad range of densities [up to $n/n_p^\sigma \sim 2$, similar to [14,15]], while it is expected to work only near the critical point [27]. However, our combined transport and compressibility measurements allow us to examine directly the applicability of the scaling procedure and demonstrate its validity. Using the NST prediction [11,13], we obtain independently $n_p \approx 0.12\sqrt{n_i}/s \approx n_m/3$ and compare it with n_p^σ. We have established that the percolation thresholds derived from both methods are very close: $n_p = 0.76 \times 10^{10}$ cm^{-2} and $n_p^\sigma = 0.7 \times 10^{10}$ cm^{-2} for H03, and $n_p = 1.2 \times 10^{10}$ cm^{-2} and $n_p^\sigma = 1 \times 10^{10}$ cm^{-2} for H05. (This comparison is done at $T = 0.26$ K and even better agreement is obtained at $T = 30$ mK as n_p^σ increases with decreasing T by about 20%.)

In summary, our combined conductance and compressibility measurements suggest that the apparent MIT in 2DHGs with r_s up to ~ 30 is neither an interaction-driven phase transition nor a percolation transition. The behavior of the compressibility at low hole densities is well described by the nonlinear screening theory. This indicates that the upturn in $\chi^{-1}(n)$ is due to depletion regions in the channel, with total area less than 3.5%, caused by disorder.

*Present address: University of New South Wales, Sydney, Australia 2052.

[1] E. Abrahams *et al.*, Rev. Mod. Phys. **73**, 251 (2001); S. V. Kravchenko and M. P. Sarachik, Rep. Prog. Phys. **67**, 1 (2004); A. A. Shashkin, Phys. Usp. **48**, 129 (2005).

[2] A. Punnoose and A. Finkel'stein, Science **310**, 289 (2005); S. Das Sarma and E. H. Hwang, Solid State Commun. **135**, 579 (2005).

[3] J. P. Eisenstein *et al.*, Phys. Rev. B **50**, 1760 (1994).

[4] S. Shapira *et al.*, Phys. Rev. Lett. **77**, 3181 (1996).

[5] S. C. Dultz and H. W. Jiang, Phys. Rev. Lett. **84**, 4689 (2000).

[6] S. Ilani *et al.*, Phys. Rev. Lett. **84**, 3133 (2000).

[7] M. Rahimi *et al.*, Phys. Rev. B **67**, 081302 (2003).

[8] Q. Si and C. M. Varma, Phys. Rev. Lett. **81**, 4951 (1998).

[9] S. Chakravarty *et al.*, Philos. Mag. B **79**, 859 (1999).

[10] A. L. Efros and B. I. Shklovskii, *Electronic Properties of Doped Semiconductors* (Springer, New York, 1984).

[11] A. L. Efros, Solid State Commun. **70**, 253 (1989); A. L. Efros, F. G. Pikus, and V. G. Burnett, Phys. Rev. B **47**, 2233 (1993).

[12] J. Shi and X. C. Xie, Phys. Rev. Lett. **88**, 086401 (2002).

[13] M. M. Fogler, Phys. Rev. B **69**, 121409(R) (2004).

[14] Y. Meir, Phys. Rev. Lett. **83**, 3506 (1999) and experiments cited therein.

[15] S. Das Sarma *et al.*, Phys. Rev. Lett. **94**, 136401 (2005).

[16] Y. Y. Proskuryakov *et al.*, Phys. Rev. Lett. **86**, 4895 (2001); **89**, 076406 (2002).

[17] H. Noh *et al.*, Phys. Rev. B **68**, 165308 (2003).

[18] R. Leturcq *et al.*, Phys. Rev. Lett. **90**, 076402 (2003).

[19] M. P. Lilly *et al.*, Phys. Rev. Lett. **90**, 056806 (2003).

[20] A. Gold and V. T. Dolgopolov, Phys. Rev. B **33**, 1076 (1986); S. Das Sarma and E. H. Hwang, Phys. Rev. Lett. **83**, 164 (1999).

[21] G. Zala, B. N. Narozhny, and I. L. Aleiner, Phys. Rev. B **64**, 214204 (2001).

[22] T. Ando, A. B. Fowler, and F. Stern, Rev. Mod. Phys. **54**, 437 (1982).

[23] M. Combescot *et al.*, Solid State Commun. **88**, 309 (1993).

[24] B. Tanatar and D. M. Ceperley, Phys. Rev. B **39**, 5005 (1989).

[25] E. Buks *et al.*, Phys. Rev. B **49**, 14 790 (1994); P. M. Koenraad *et al.*, Superlattices Microstruct. **21**, 237 (1997); N. B. Zhitenev *et al.*, Nature (London) **404**, 473 (2000).

[26] P. Grassberger, Physica (Amsterdam) **262A**, 251 (1999).

[27] A. Gold, Phys. Rev. B **44**, 8818 (1991).